Research Square

Preprints are preliminary reports that have not undergone peer review.
They should not be considered conclusive, used to inform clinical practice,
or referenced by the media as validated information.

Pharmacological Inhibition of USP7 Supresses Growth and Metastasis of Melanoma Cells in Vitro and in Vivo

Minmin Xiang
Xiangya Hospital Central South University
Long Liang
Xiangya Hospital Central South University
Xinwei Kuang
Xiangya Hospital Central South University
Zuozhong Xie
Xiangya Hospital Central South University
Jing Liu
Central South University
Shuang Zhao
Xiangya Hospital Central South University
Juan Su
Xiangya Hospital Central South University
Xiang Chen
Xiangya Hospital Central South University
Hong Liu (hongliu1014@csu.edu.cn)
Department of Dermatology, Xiangya Hospital, Central South University, Changsha, Hunan, 410008, China.

Research

Keywords: Melanoma, USP7, Apoptosis, ROS, Invasion

Posted Date: December 3rd, 2020

DOI: https://doi.org/10.21203/rs.3.rs-117715/v1

License: This work is licensed under a Creative Commons Attribution 4.0 International License.
Read Full License

Abstract

Background: Melanoma is a highly aggressive type of skin cancer. Due to the development of diverse resistance mechanisms and severe adverse side effects, significantly limits the efficiency of current therapeutic approaches. Identification of the new therapeutic targets involved in the pathogenesis will benefit to develop novel therapeutic strategies. The deubiquitinase USP7(ubiquitin-specific protease-7) is deregulated in serval cancer types, as a potential target for cancer treatment, but its role in melanoma is still unclear. Here, we investigated the role of USP7 and its inhibitor P22077 in melanoma treatment.

Methods: To explore the role of USP7 and the anti-tuomr effect of P22077 in melanma progression and metastasis, a series of cell biological, molecular and biochemical approaches were used for in vitro and in vivo investigations.These methods included RT-qPCR, Western blot assay, cell transfection, CCK8 assay, flow cytometry, scratch test, Transwell assay, mouse xenograft,TUNEL staining.

Results:The USP7 inhibitor P22077 suppressed the growth of melanoma in vitro and in vivo. additionally, P22077 induction of cell cycle arrest and apoptosis via ROS(reactive oxygen species) accumulation-induced DNA damage. Furthermore, inhibition of USP7 also prevented migration and invasion of melanoma cells in vitro and in vivo by decrease the Wnt/β-catenin signal pathway.

Conclusion: Our data indicated that USP7 acts as an oncogene involved in melanoma cell proliferation and metastasis and may provide a novel therapeutic target for melanoma treatment.

Background

Melanoma, representing the most aggressive and the deadliest type of skin cancer, a malignancy originating from the neural crest-derived melanocytes in skin, uvea and mucosal tissue [1]. The incidence rate of melanoma is lower than many common cancers worldwide, such as lung cancer, liver cancer and colorectal cancer, but the number of melanoma cases is increasing faster than any other type of cancer [2]. Besides melanoma has unusual age demography, which caused particular concern. Unlike other solid malignancies, where the majority of cases are diagnosed at over the age of 65, melanoma affects a higher proportion of younger patients, with a median age of diagnosis of 57 years [3]. Although timely recognition, detection and appropriate surgery improved the outcomes, the prognosis of metastatic melanoma remains poor [4]. More than 95% of melanoma patients with three or more sites of the metastatic disease die within 1 year [5]. 75% of melanoma patients usually suffer from brain metastasis and brain metastases cause death in 95% of total cases[6]. Over the past years, the inauguration of several novel systematic therapies such as BRAF-targeted therapy and immunotherapy, and advancement in local therapy have contributed for improving survival rate [7]. Unfortunately, a large fraction of patients fail to benefit from these targeted therapies due to the skin and gastrointestinal toxicity and low efficiency, only a minority of patients responding to the treatments[8]. Therefore, there is an urgent need to figure out the disease pathogenesis to find new therapeutic targets and develop new drugs with low toxicity for melanoma treatment.

Ubiquitination is an important type of protein post-translational modification (PTM) which plays a crucial role in controlling substrate degradation to ensure protein homeostasis in the cell [9]. Deubiquitinases (DUBs) can reverse the effect of E3 ligases to remove ubiquitin from ubiquitylated proteins to regulate the stability, subcellular localization, or activity of modified proteins[10]. The role of DUBs in cancer is multifaceted, involved in proliferation, cell cycle control, apoptosis, the DNA damage response, etc. USP7 is one of the deubiquitinases belong to the ubiquitin(UBQ)-specific proteases family and plays critical roles in cancers, neurological disorders, cell differentiation, immune dysfunction, etc[11, 12]. USP7 activity is highly context-specific and exhibits its versatility in substrate selection. The multifaceted role of USP7 in various cancers is established, including lung cancer, colon cancer, breast cancer, leukemia, etc[13]. Studies revealed numerous substrates of USP7 and demonstrated that the USP7 exhibits oncogenic properties. These findings make USP7 as an attractive target for pharmacological discoveries and specific treatment strategy designs[14]. However, the role of USP7 and its therapeutic value for melanoma remains unclear.

P22077 is a specific USP7 inhibitor which has been identified by activity-based chemical proteomics [15]. P22077 inhibits neuroblastoma and colon carcinoma growth via inducing p53-mediated apoptosis[16]. Current studies have also shown that USP7 suppressed proliferation and the colony formation capacity of lung cancer cells [17]. However, the antitumor effect of P22077 in melanoma has not yet been studied.

Here, we found a high expression of USP7 in melanoma patients that correlates the poor overall survival. Further, using P22077 to inhibit USP7 demonstrated a suppression in the cell growth and induction of cell cycle arrest and apoptosis via ROS accumulation-induced DNA damage. Moreover, P22077 also suppressed the metastasis of melanoma cells by inhibiting β-catenin. These data indicate that USP7 inhibition could be a potential strategy for melanoma treatment.

Materials And Methods

Human melanoma tissue microarray

Human melanoma tissue microarray (malignant melanoma with skin tissue array,80 cores) was purchased from www.alenabio.com Immunohistochemistry (IHC) staining assays using anti-human USP7 antibody(1:1000,ab4080,abcam) were performed following standard protocols (Wuhan Servicebio Technology Co., Ltd., Hubei, China) and slides scanned using an automatic digital slide scanner (Pannoramic MIDI II,). The density quantified by using quant software (3D Histech), and the histochemistry score (H-score) system were used to assess the protein levels.

Reagents and antibodies

P22077 was purchased from Selleck(S713301).HDM2 (86934), P-ATR(30632), ATM (2873)P-ATM(13050), P-ATR (30632),γ-H2AX(9718),MMP9(13667),Vimentin(5741), β-catenin(8480),CyclinB(12231) antibodies were purchased from Cell Signaling (Cell Signaling Technology, Danvers, MA, USA). USP7(ab4080),caspase-3(ab13847) ,cleaved-caspase-3(ab214430)antibodies were

purchased from abcam, ATR (19787-1-AP), cCdc-2 (27334-1-AP),P-cCdc-2(21082-1-AP),GAPDH(60004-1-Ig) antibodies were purchased from Protech)

Cell lines and cell culture

The human malignant melanoma cell lines A375, Sk-Mel-28 were maintained in Dulbecco's modified Eagle's medium(DMEM) (BI, Israel) supplemented with 10% heat-inactivated fetal bovine serum (FBS) (BI, Israel), 100 units/ml penicillin, 100 μg/ml streptomycin, and 2 mM glutamine. The mouse cell line B16F10 was maintained in Roswell Park Memorial Institute(RPMI) 1640 containing 10% FBS, 100 units/ml penicillin, 100 μg/ml streptomycin, and 2 mM glutamine. All cells were grown in a humidified incubator containing 5% CO_2 at 37 °C.

Cell viability assay

Cell viability assays were assessed by the Cell Counting Kit-8 reagent (Selleck,USA) following the manufacturer's instructions. Cells were seeded into 96-well plates (2.5×10^3 cells per well) and incubated overnight. Then cells were cultured in various concentrations of P22077 or Dimethyl sulfoxide(DMSO) (control). 24, 48 and 72 hours later, 10 μl of CCK-8 was added into each well and after 2h of incubation, the absorbance was measure at 450 nm using the spectrophotometer (Beckman, USA). Each experiment was performed 6 replicates.

Apoptosis and cell cycle analysis

Cells were seeded into 6-well plates (3×10^5 cells per well) and incubated overnight at 37 °C in media containing 10% FBS with various concentrations of P22077 or DMSO (control). For cell cycle assays, the cells were harvested by trypsinization after 48 h. The cells were re-suspended in 300 μl Phosphate Buffered Saline(PBS), and subsequently add 700ul 100% ethanol to the cell suspension. After incubation at 4°C.

for at least overnight, PBS wash the cells three times.The next day, according to the manufacturer's instructions, the collected cells were incubated at room temperature in the dark with propidium iodide (PI) , (Becton Dickinson and Company (USA)).The cell cycle profile was analyzed using a flow cytometer(BD)For apoptosis assays, cells were harvested after 48 hours by trypsin digestion without EDTA. The collected cells were washed with cold PBS and incubated with an Annexin V / propidium iodide stain (Becton, Dickinson and Company, US) , according to the manufacturer. Cell Apoptosis was detected by Flow cytometry and analyzed using FlowJo software.

Wound healing

5×10^5 cells/well were seeded into six-well plates and incubated under standard conditions overnight. The cells reached confluence using a 1000 μL pipette tip to scraping the cell monolayer create a wound. cells

were treated with various concentrations of P22077 or DMSO (control) and photomicrographs were taken at 0 h and 24 h. Representative images were captured using an inverted light microscope.

Transwell chamber Invasion and migration assay

Place the Transwell chamber into the corresponding culture plate. The upper chamber contains the serum-free medium and corresponding P22077 or DMSO(control), the lower chamber contains media containing 30% FBS. Seed the melanoma cells in the upper chamber. After 24 h, the cells were fixed with 4% PFA and stained by 0.1% crystal violet, migrated cell number was counted by phase contrast microscope and statistically analyzed. To perform the invasion assay, transwell chambers were precoated with ECM Matrix gel solution (Sigma-Aldrich, USA) for 24 h. Residual cells on the upper transwell chambers were counted and statistically analyzed in five random fields per chamber.

Immunoblotting

Collect cells treated with P22077 or DMSO for 48 hours, add 200ul of PMSF-containing lysate to each sample and lyse on ice for 30 min. Centrifuge at 12000 rpm for 5 min at 4 ° C and collect the supernatant.Then use the BCA protein assay kit (Beyotime, China) to measure protein concentration. Protein detection followed Standard SDS-polyacrylamide gel electrophoresis(SDS-PAGE) andimmunoblotting protocols and incubated with primary and secondary antibodies.

Detection of intracellular ROS generation

Cells were seeded into 6-well plates (3×10^5 cells per well) and incubated overnight at 37 °C in medium containing 10% FBS treated with P22077 or DMSO (control). The cells were processed with 2,7-Dichlorodi-hydrofluorescein diacetate(DCFH-DA) incubated for 20 minutes according to the manufacturer's instructions, and then the intracellular fluorescence intensities were detected using a flow cytometer and analyzed by FlowJosoftware.

Xenograft tumor model

1×10^6 A375 cells surgically injected into the left renal capsule of 5-week-old female SD nude mice. The xenografts were allowed to grow for 2 weeks before randomizing the mice into a control group and a P22077 treatment group. Animals were treated with DMSO or P22077 by intraperitoneal (i.p.) injection every day for 14 days. At the end of the experiments, all mice were sacrificed and weighed and photographed.

Syngeneic lung tumor metastasis models

5×10^5 B16F10 cells were injected into the tail veins of 6- to 8-week-old C57B6 mice maintained under specific pathogen–free conditions. Animals were treated with DMSO or P22077 by intraperitoneal (i.p.) injection every day for 16 days. At the endpoint the mice were killed by CO_2 asphyxiation, the lung tumors were counted, and lung images were captured.

Statistical analysis

Student’s t-tests and one- or two-way ANOVA tests were conducted to analyze

the data using the GraphPad Prism software (version 6.01). The quantified dataare presented as the mean ± SEM. Differences were considered to be significantwhen $p < 0.05$.

Results

USP7 is overexpressed and correlates with poor prognosis in melanoma.
To explore the relationship between USP7 and malignancy of melanoma, first, we examined the expression levels of USP7 in a human tissue microarray comprising 40 melanoma specimens from 40 patients (23 female, 17 male, ages15-80; mean 55). The histochemical staining images were randomly selected which showed the USP7 expression level (Figure 1A and 1B). The USP7 expression significantly elevated in 77.5 % of all melanomas (31/40), whereas USP7 expression was significantly lower in non-malignant melanocytes (Figure 1C). Besides, compared to the normal epithelial cells, the USP7 protein level was also higher in melanoma cell lines (Figure 1D). Next, we analyzed the USP7 expression in melanoma form TCGA data programed online tool GEPIA and found that tumors with higher USP7 expression correlate with poor overall survival in melanoma(Figure 1E). Altogether, these results demonstrate that USP7 expression is elevated in melanoma and is correlated with patients' poor outcomes.
Pharmacological inhibition of USP7 by P22077 inhibits proliferation and induces cell cycle arrest and apoptosis in melanoma cells.
To evaluate the potential therapeutic role of USP7 inhibition in melanoma, we treated the TP53-mutated melanoma cell line SK-Mel-28 and wild type cell line A375 with P22077. P22077 treatment significantly suppressed the proliferation of A375 and SK-Mel-28 cells in a dose-dependent manner but caused no cytotoxic effect on normal human skin keratinocytes cell line (HaCat) (Figure 2A). To investigate the effect of P22077-induced cytotoxicity in melanoma cells, we analyzed the apoptosis and cell cycle status in A375 and SK-Mel-28 cell lines. P22077 inhibited the proliferation of A375 and SK-Mel-28 cells by increasing the percentage of cells in G2/M and decreased the percentage of cells in G0/G1 and S phase (Figure 2B). This was confirmed by specific cell cycle protein signaling with reduced phosphorylation of cell cycle regulatory proteins Cdc2 and cyclin B (Figure 2C). We also found that USP7 inhibition increased significantly early (Annexin+/PI−) and late apoptosis (Annexin+/PI+) regardless of P53 status (Figure 2D). Apoptosis was further confirmed by immunoblotting showing induction of the cleavage of Caspase-3. At the same time, the inhibition efficiency of P22077 was confirmed by HMD2, the known substrate of USP7 (Figure 2E). Together, the results suggest that USP7 inhibitor P22077 potentially induces cell cycle arrest and apoptosis in melanoma cell lines independent of the TP53 status.

P22077 induced DNA damage by increasing intracellular ROS level in melanoma cells.
At moderate levels, ROS contributes to tumor growth by acting as signaling molecules or promoting the mutation of genomic DNA, but ROS overload also prompts oxidative damage to biomacromolecules in

the cell, which leads to cell dysfunction and death. Based on the previous results, which showed that P22077 treatment suppressed proliferation and induced apoptosis in melanoma cells, We hypothesized that P22077 elevates ROS levels to induce melanoma cell cycle arrest and apoptosis. We applied flow cytometry to assessed ROS level by intracellular DCF fluorescence and found a significant and dose-dependent increase of intracellular levels of ROS in melanoma cell lines after an increasing concentration of P22077 treatment (Figure 3A). ROS generation is well-known to lead DNA damage and subsequently antitumor activity. ATM and ATR play critical roles in DNA damage responses, this checkpoint pathways are activated by ROS-induced DNA damage. In melanoma cell lines, P22077 treatment remarkably activated the ATM/ATR signaling pathway. The results showed that P22077 induced the upregulation of p-ATM, p-ATR and γH2AX expression levels (Figure 3B). These data indicate that the anti-melanoma effect of P22077 is mediated through DNA damage induced by intracellular ROS.

P22077 significantly inhibits melanoma tumor growth in vivo.

Next, we investigate the in vivo antitumor effect of P22077. First, the melanoma cell line A375 used to create a subcutaneous xenograft model in nude mice. The tumor-bearing mice were treated with vehicle and P22077(10mg/kg) by intravenous (IV) injection for 14 days (Figure 4A). The results showed that P22077 treatment reduced the mouse tumor growth rate without body weight changes, indicating the safety of the P22077 treatment group (Figure 4 B and C). Both tumor size and tumor weight were significantly decreased in the P22077-treated group compared with the vehicle group (Figure 4 D and E). Further, The HE staining revealed a relatively much higher density of necrotic cells in P22077-treated xenograft tumor sections compared to the control group (Figure 4F). The TdT-mediated dUTP nick-end labeling (TUNEL) assay showed that the percentage of apoptotic tumor cells was increased in the P22077 group compared with the vehicle group(Figure 4G). These results demonstrate the efficacy of P22077 in inhibiting in vivo tumor growth without toxicity at therapeutic doses.

P22077 inhibits metastasis and invasion in melanoma in vitro and in vivo.

The epithelial-mesenchymal transition (EMT) is a key process for promoting tumor cell invasion and metastasis[18]. Based on the aforementioned results, we evaluated the effect of P22077 on the capability of migration by performing a Wound-healing assay. The results revealed a decreased closure of the wound area compared with control cells after P22077 treatment (Figure 5A). Next, the effect of USP7 inhibition on the invasive ability of cells was accessed by transwell assays. P22077 showed a dramatic attenuation of the invasive capacities of A375 and SK-Mel-28 cells compared with untreated cells (Figure 5B). To further explore the underlying molecular mechanism of the P22077 effect on the EMT, the EMT associated protein markers were examined after P22077 treatment. The results demonstrated that the inhibition of USP7 significantly induced the expression of the epithelial marker snail and reduced the mesenchymal markers vimentin and MMP9 significantly (Figure 5C). The expression of β-catenin a key nuclear effector of canonical Wnt signaling was also downregulated, which implied that P22077 could inactivate the Wnt/β-catenin pathway to inhibit EMT (Figure 5C). To further demonstrate the effect of P22077 on melanoma metastasis, we applied the B16-F10 cells Injection through the lateral tail vein to induce melanoma lung metastasis in C57BL/6 mice. The results showed that after P22077 treatment the

lung metastases were decreased significantly and without toxicity (Figure 6 A-C). These findings suggest that P22077 exerts antimetastatic activity in vitro and in vivo.

Discussion

Melanoma is one of the most malignant diseases worldwide, the most aggressive and deadliest type of skin cancer[19]. Uncontrolled tumor growth and distant metastasis remain huge obstacles to effective treatments. Despite the favorable results were obtained from immunotherapy, in general, only a small subset of patients showed a promising response. To identify novel targets that contribute to the growth and metastasis of melanoma to develop innovative strategies still needed. In this study, we found that a notable number of melanoma patients contain high USP7 expression which correlates with reduced overall survival. Pharmacological inhibition of USP7 by P22077 reduces melanoma cell proliferation and induces cell cycle arrest and apoptosis in independent of the TP53 status. The anti-melanoma activity of P22077 might be mediated through induced intracellular ROS leading to DNA damage and subsequent cell death. P22077 was also active without toxicity at a therapeutic dose against melanoma xenograft and inhibits invasion and metastasis of melanoma cells in vitro and in vivo. Our data suggest that targeting USP7 would provide a potential strategy for melanoma treatment.
USP7 is the most widely studied deubiquitinating enzyme with numerous substrates including viral proteins, transcription factors, and epigenetic modulators[20]. In a wide variety of cancers, USP7 acts as an oncogene, and the high expression of USP7 leads to the progression of cancer and as a good therapeutic target for cancer[21]. But, USP7 assumes play a variety of roles in tumors through the stabilization of different substrates. For example, the tumor suppressor protein p53 was the first identified deubiquitination substrate for USP7, this attributed to USP7 as a tumor suppressor, given its ability to increase the stability of p53, resulting in repress cancer cell growth and activation of apoptotic pathways[22]. A later study showed the p53 E3-ligase mouse double minute 2 homolog (MDM2) is also regulated by USP7-mediated deubiquitination, leading to the degradation of p53 and reversal of the above mentioned cellular phenotype[23]. Though, in normal conditions without DNA damage induction, the USP7 has a higher affinity with MDM2[24]. Our data showed an increase in USP7 levels in melanoma cells independent of TP53 status which indicated that USP7 may active through other substrates to act as an oncogene in melanoma. Previous studies also have shown that USP7 regulates serval substrates to promotes carcinogenesis independent of p53. These include controlling subcellular localization of phosphatase and tensin homolog deleted on chromosome ten(PTEN) to promotes acute megakaryoblastic leukemia(AML) progression, stabilization of the histone demethylase PHD Finger Protein 8(PHF8) to promotes breast carcinogenesis, stabilization of N-Myc to promotes neuroblastoma progression among others[25-27]. Though we found an oncogenic role of USP7 with melanoma, nonetheless, the substrate requirement for USP7 to promote the progression in melanoma required further exploration.

USP7 is a promising anticancer therapeutic target because of its aberrant expression and the oncogenic role in various cancers. There are various small-molecular inhibitors such as HBX41108, P5091, FT671, and P22077 that have been reported to inhibit USP7 in cells[24, 28-30]. In recent years, several groups

reported the structures of USP7 in complex with small molecule inhibitors [24, 31]and these structures give guidance to further develop new inhibitors. The P22077 covalently modifies the catalytic cysteine of USP7 and induce a conformational switch in the enzyme associated with active site rearrangement[32]. This makes P22077 well-characterized tool compounds for exploring the USP7 function[33]. In melanoma P22077 induced an excessive ROS, further leads to DNA damage. The excessive amounts of ROS enhance cellular oxidative stress and directly activate ATM, and ATR for the DNA damage response pathway[34]. Previous studies have shown that USP7 act as an important regulator for DNA damage response, inhibition or knockdown USP7 leads to increased DNA damage via destabilization of serval regulators of DNA damage include RAD18 (replication-associated repair), CSB (nucleotide excision repair), and ALKBH2/3 (alkylation repair)[35-37]. Moreover, USP7 also induced unfolded protein accumulation causing ER stress in cancer cells, which leads to oxidative stress to induce DNA damage. On the other hand, we also found that P22077 lead inhibition of invasion and migration in vitro and in vivo in melanoma. Several substrates contribute to invasion and migration regulated by USP7, such as EZH2 in prostate cancer, LSD1 in glioblastoma[38, 39]. Contrary, the role of ROS in triggering signaling pathways, such as activation of MAPK, ERK, JNK, and p-38 MAPK via growth factor-mediated stimulation of receptor tyrosine kinases (RTKs) for cell migration and invasion has been well-established[40]. Those studies indicated USP7 as a multifaceted regulator of tumorigenesis that may act through different mechanisms at the same time.

Conclusion

This study demonstrated USP7 as a possible oncogenic molecule for melanoma progression, and inhibition of USP7 might be a potential strategy for the suppression of melanoma growth. Importantly, USP7 inhibitor P22077 posses anti-melanoma activities in vitro and in vivo, induces apoptosis and cell cycle arrest by DNA damage and markedly impaired melanoma cell migration and invasion, indicating a prospective value of the application of P22077 as a promising novel effective way for melanoma therapy.

List Of Abbreviations

AML acute megakaryoblastic leukemia

CCK8 Cell counting kit-8

DCFH-DA 2,7-Dichlorodi -hydrofluorescein diacetate

DMEM Dulbecco’s modified Eagle’s medium

DMSO Dimethyl sulfoxide

DUBs Deubiquitinases

FBS fetal bovine serum

H-score histochemistry score

IHC Immunohistochemistry

MDM2 E3-ligase mouse double minute 2 homolog

PBS Phosphate Buffered Saline

PTM post-translational modification

PTEN phosphatase and tensin homolog deleted on chromosome ten

PHF8 PHD Finger Protein 8

RTKs receptor tyrosine kinases

RPMI Roswell Park Memorial Institute

SDS-PAGE SDS-polyacrylamide gel electrophoresis

UBQ ubiquitin

USP7 ubiquitin-specific protease-7

Declarations

Ethics approval and consent to participate

The animal protocol was approved by the Ethics Committee of Xiangya Hospital (Central South University, China).

Consent for publication

Not applicable.

Availability of data and materials

Not applicable.

Competing interests

The authors declare no conflict of interest.

Funding

This study was supported by the National Natural Science Foundation of China (No.81874242, No.31800979), National Key Research and Development Program of China (2019YFA0111600), the Natural Science Foundation of Hunan Province for outstanding Young Scholars (No.2019JJ30040), Natural Science Foundation of Hunan Province of China 2018SK2082 2020JJ4884, Scientific Research Project of Hunan Health and Family Planning Commission(B20180855), Innovation-driven Talent Project of Central South University(No.502501008), High-level Talent Plan of Xiangya Hospital of Central South University(No.2209090550043), Overseas Expertise Introduction Project for Discipline Innovation: 111 Project, No. B20017.

Authors' contributions

HL and XC designed this study. MMX and LL performed the experiment and wrote the manuscript. XWK, JL and ZZX conducted the animal experiment and revised the manuscript. JS and SZ performed the statistical analyses. All authors read and approved the final manuscript.

Acknowledgements

The authors would thank the members of the Hunan Key Laboratory of Skin Cancer and Psoriasis and the Hunan Engineering Research Center of Skin Health and Disease, Xiangya Hospital, Central South University for constructive discussion of this study.

References

[1]. Shain, A.H. and B.C. Bastian, From melanocytes to melanomas. Nat Rev Cancer, 2016. 16(6): p. 345-58.

[2]. Ferlay, J., et al., Cancer incidence and mortality worldwide: sources, methods and major patterns in GLOBOCAN 2012. Int J Cancer, 2015. 136(5): p. E359-86.

[3]. Ali, Z., N. Yousaf and J. Larkin, Melanoma epidemiology, biology and prognosis. EJC Suppl, 2013. 11(2): p. 81-91.

[4]. Pavri, S.N., et al., Malignant Melanoma: Beyond the Basics. Plast Reconstr Surg, 2016. 138(2): p. 330e-40e.

[5]. Damsky, W.E., N. Theodosakis and M. Bosenberg, Melanoma metastasis: new concepts and evolving paradigms. Oncogene, 2014. 33(19): p. 2413-22.

[6]. Nicholas, S., et al., Metastatic melanoma to the brain: surgery and radiation is still the standard of care. Curr Treat Options Oncol, 2013. 14(2): p. 264-79.

[7]. Rishi, A. and H.M. Yu, Current Treatment of Melanoma Brain Metastasis. Curr Treat Options Oncol, 2020. 21(6): p. 45.

[8]. Mishra, H., et al., Melanoma treatment: from conventional to nanotechnology. J Cancer Res Clin Oncol, 2018. 144(12): p. 2283-2302.

[9]. Swatek, K.N. and D. Komander, Ubiquitin modifications. Cell Res, 2016. 26(4): p. 399-422.

[10]. Kim, R.Q. and T.K. Sixma, Regulation of USP7: A High Incidence of E3 Complexes. J Mol Biol, 2017. 429(22): p. 3395-3408.

[11]. Zhou, J., et al., USP7: Target Validation and Drug Discovery for Cancer Therapy. Med Chem, 2018. 14(1): p. 3-18.

[12]. Kim, R.Q. and T.K. Sixma, Regulation of USP7: A High Incidence of E3 Complexes. J Mol Biol, 2017. 429(22): p. 3395-3408.

[13]. Cai, J.B., et al., Ubiquitin-specific protease 7 accelerates p14(ARF) degradation by deubiquitinating thyroid hormone receptor-interacting protein 12 and promotes hepatocellular carcinoma progression. Hepatology, 2015. 61(5): p. 1603-14.

[14]. Nicholson, B. and K.K. Suresh, The multifaceted roles of USP7: new therapeutic opportunities. Cell Biochem Biophys, 2011. 60(1-2): p. 61-8.

[15]. Altun, M., et al., Activity-based chemical proteomics accelerates inhibitor development for deubiquitylating enzymes. Chem Biol, 2011. 18(11): p. 1401-12.

[16]. Fan, Y.H., et al., USP7 inhibitor P22077 inhibits neuroblastoma growth via inducing p53-mediated apoptosis. Cell Death Dis, 2013. 4: p. e867.

[17]. Li, J., et al., The m6A demethylase FTO promotes the growth of lung cancer cells by regulating the m6A level of USP7 mRNA. Biochem Biophys Res Commun, 2019. 512(3): p. 479-485.

[18]. Turley, E.A., et al., Mechanisms of disease: epithelial-mesenchymal transition–does cellular plasticity fuel neoplastic progression? Nat Clin Pract Oncol, 2008. 5(5): p. 280-90.

[19]. Schadendorf, D., et al., Melanoma. Lancet, 2018. 392(10151): p. 971-984.

[20]. Peng, Y., et al., USP7 is a novel Deubiquitinase sustaining PLK1 protein stability and regulating chromosome alignment in mitosis. J Exp Clin Cancer Res, 2019. 38(1): p. 468.

[21]. Georges, A., et al., Identification and Characterization of USP7 Targets in Cancer Cells. Sci Rep, 2018. 8(1): p. 15833.

[22]. Wang, M., et al., The USP7 Inhibitor P5091 Induces Cell Death in Ovarian Cancers with Different P53 Status. Cell Physiol Biochem, 2017. 43(5): p. 1755-1766.

[23]. An, T., et al., USP7 inhibitor P5091 inhibits Wnt signaling and colorectal tumor growth. Biochem Pharmacol, 2017. 131: p. 29-39.

[24]. Kategaya, L., et al., USP7 small-molecule inhibitors interfere with ubiquitin binding. Nature, 2017. 550(7677): p. 534-538.

[25]. Carra, G., et al., Therapeutic inhibition of USP7-PTEN network in chronic lymphocytic leukemia: a strategy to overcome TP53 mutated/deleted clones. Oncotarget, 2017. 8(22): p. 35508-35522.

[26]. Wang, Q., et al., Stabilization of histone demethylase PHF8 by USP7 promotes breast carcinogenesis. J Clin Invest, 2016. 126(6): p. 2205-20.

[27]. Tavana, O., et al., HAUSP deubiquitinates and stabilizes N-Myc in neuroblastoma. Nat Med, 2016. 22(10): p. 1180-1186.

[28]. Chauhan, D., et al., A small molecule inhibitor of ubiquitin-specific protease-7 induces apoptosis in multiple myeloma cells and overcomes bortezomib resistance. Cancer Cell, 2012. 22(3): p. 345-58.

[29]. Reverdy, C., et al., Discovery of specific inhibitors of human USP7/HAUSP deubiquitinating enzyme. Chem Biol, 2012. 19(4): p. 467-77.

[30]. Zhang, Y., et al., Conformational stabilization of ubiquitin yields potent and selective inhibitors of USP7. Nat Chem Biol, 2013. 9(1): p. 51-8.

[31]. Turnbull, A.P., et al., Molecular basis of USP7 inhibition by selective small-molecule inhibitors. Nature, 2017. 550(7677): p. 481-486.

[32]. Pozhidaeva, A., et al., USP7-Specific Inhibitors Target and Modify the Enzyme's Active Site via Distinct Chemical Mechanisms. Cell Chem Biol, 2017. 24(12): p. 1501-1512.e5.

[33]. Pozhidaeva, A., et al., USP7-Specific Inhibitors Target and Modify the Enzyme's Active Site via Distinct Chemical Mechanisms. Cell Chem Biol, 2017. 24(12): p. 1501-1512.e5.

[34]. Srinivas, U.S., et al., ROS and the DNA damage response in cancer. Redox Biol, 2019. 25: p. 101084.

[35]. Zlatanou, A., et al., USP7 is essential for maintaining Rad18 stability and DNA damage tolerance. Oncogene, 2016. 35(8): p. 965-76.

[36]. Zhu, Q., et al., USP7-mediated deubiquitination differentially regulates CSB but not UVSSA upon UV radiation-induced DNA damage. Cell Cycle, 2020. 19(1): p. 124-141.

[37]. Zhao, Y., et al., Noncanonical regulation of alkylation damage resistance by the OTUD4 deubiquitinase. EMBO J, 2015. 34(12): p. 1687-703.

[38]. Lee, J.E., C.M. Park and J.H. Kim, USP7 deubiquitinates and stabilizes EZH2 in prostate cancer cells. Genet Mol Biol, 2020. 43(2): p. e20190338.

[39]. Yi, L., et al., Stabilization of LSD1 by deubiquitinating enzyme USP7 promotes glioblastoma cell tumorigenesis and metastasis through suppression of the p53 signaling pathway. Oncol Rep, 2016. 36(5): p. 2935-2945.

[40]. Rodic, S. and M.D. Vincent, Reactive oxygen species (ROS) are a key determinant of cancer's metabolic phenotype. Int J Cancer, 2018. 142(3): p. 440-448.

Figures

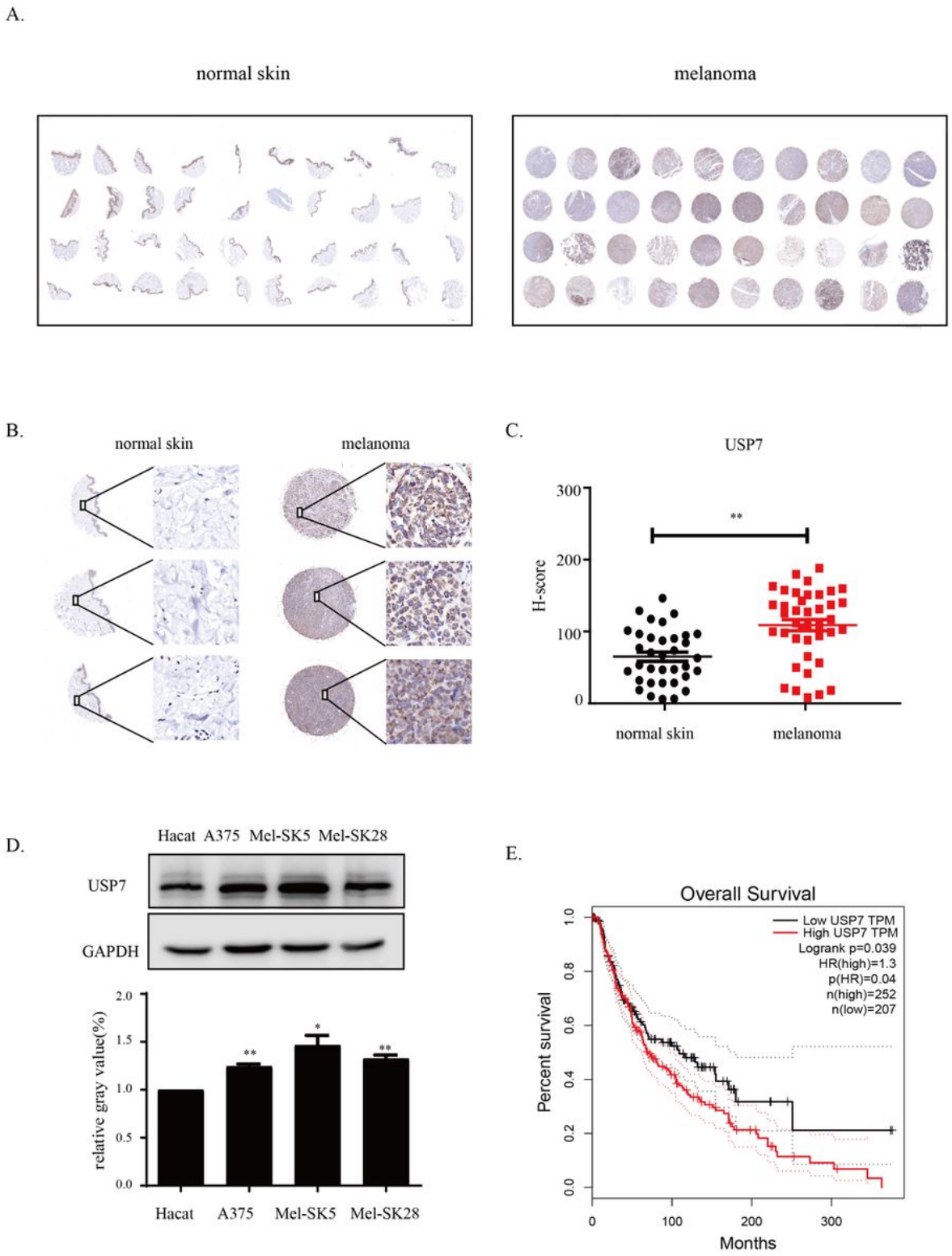

Figure 1

USP7 is overexpressed and correlates with poor prognosis in melanoma. immunohistochemical staining of USP7 in normal skin and malignant melanoma. The whole scanned image of the tissue array. B. magnified view of a tissue microarray disk with USP7 staining indicated that USP7 was highly expressed in melanoma tissues. Representative images (200× magnification).Scale bar, 50μm. C. The USP7 H-score was determined by 3D Histech Quant Center and presented as dots plots. (**P < 0.01); D. The protein level

of USP7 in the human skin keratinocytes cell line (Hacat) and different melanoma cell lines were measured by Western blot. Quantitative analysis of USP7 protein expression compared with Hacat cell; Significant differences were evaluated using Student's t-test. *p< 0.05 vs Hacat cell. E. Kaplan-Meier survival analysis for the relationship between survival time of melanoma patients and the mRNA expression level of USP7 from GEPIA. (cut off TPM 45%).

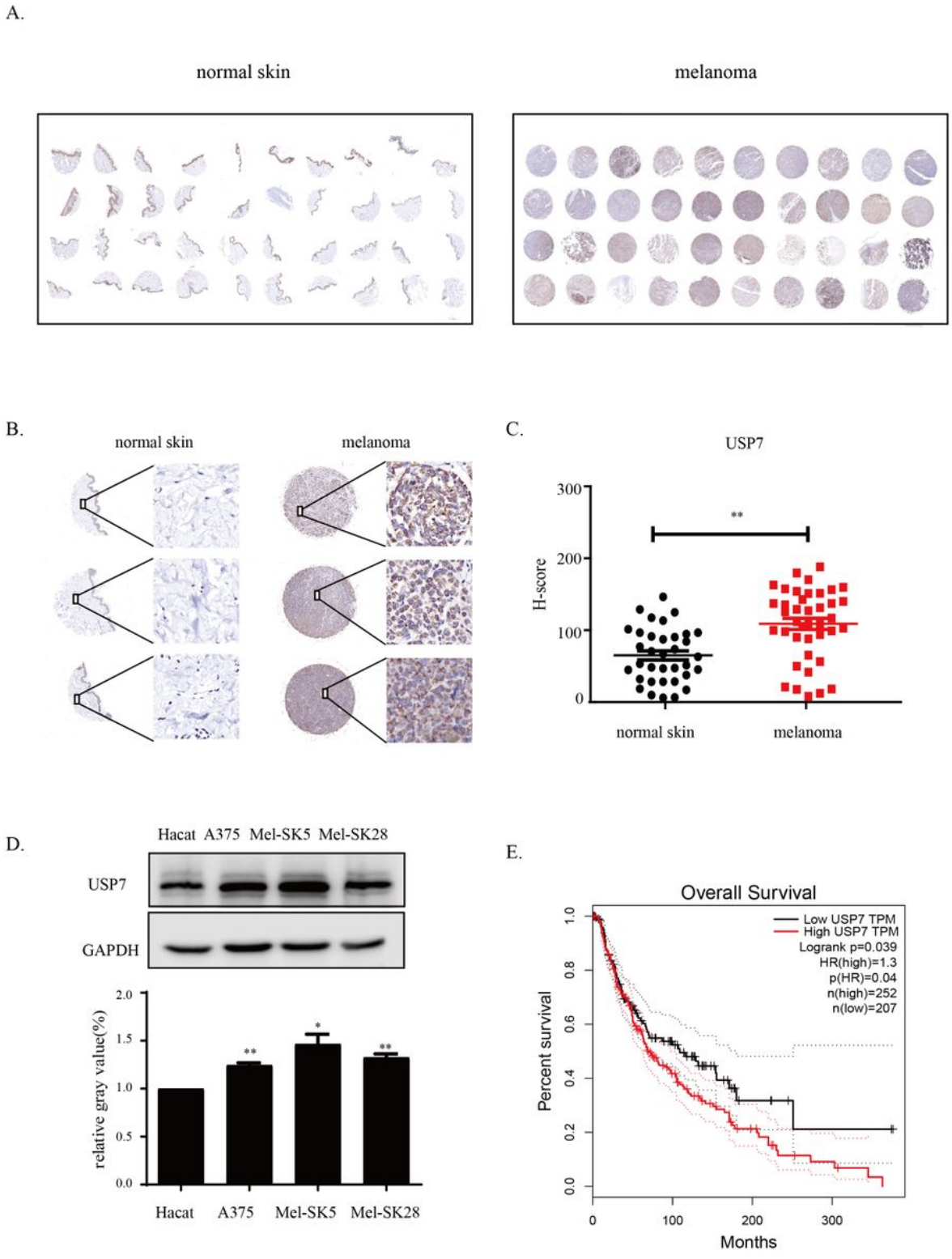

Figure 1

USP7 is overexpressed and correlates with poor prognosis in melanoma. immunohistochemical staining of USP7 in normal skin and malignant melanoma. The whole scanned image of the tissue array. B. magnified view of a tissue microarray disk with USP7 staining indicated that USP7 was highly expressed in melanoma tissues. Representative images (200× magnification).Scale bar, 50μm. C. The USP7 H-score was determined by 3D Histech Quant Center and presented as dots plots. (**P < 0.01); D. The protein level of USP7 in the human skin keratinocytes cell line (Hacat) and different melanoma cell lines were measured by Western blot. Quantitative analysis of USP7 protein expression compared with Hacat cell; Significant differences were evaluated using Student's t-test. *p< 0.05 vs Hacat cell. E. Kaplan-Meier survival analysis for the relationship between survival time of melanoma patients and the mRNA expression level of USP7 from GEPIA. (cut off TPM 45%).

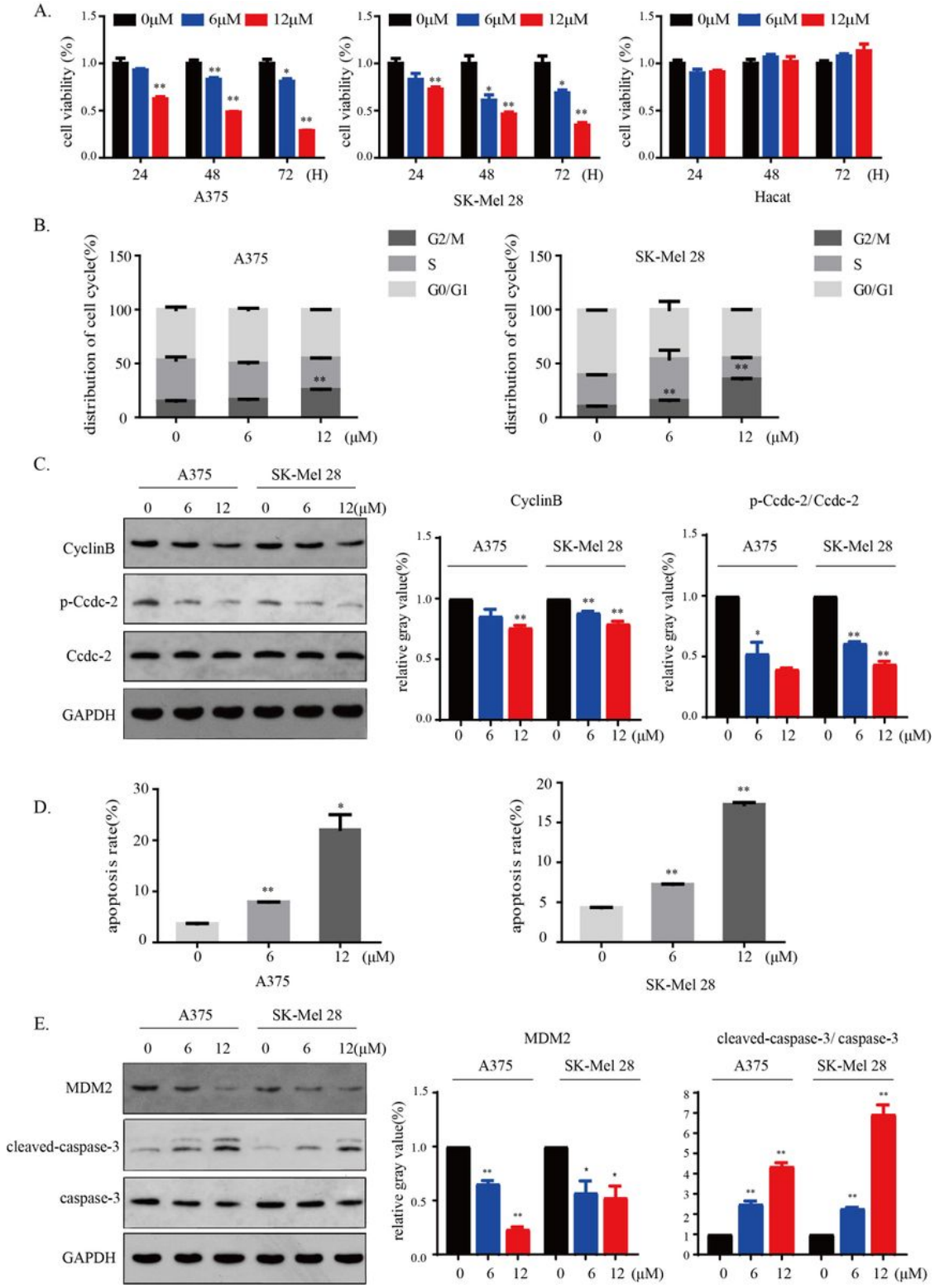

Figure 2

Pharmacological inhibition of USP7 by P22077 inhibits proliferation and induces cell cycle arrest and apoptosis in melanoma cells. A. The cell viability of melanoma cell lines in the presence or absence of USP7 inhibitor P22077. Cellsurvival was scored in triplicate normalized to control. Values are expressed asmean and SD from three independent experiments (*p<0.05, **p<0.01). B.A375 and Sk-Mel-28 cells were treated with different dosages of P22077 for 48h. The cell cycle distribution was detected by flow

cytometry. Significant differences were evaluated using Student's t-test. *p < 0.05 vs control. C. Whole cell lysates after treatment with the indicated concentration of P22077 were subjected to immunoblotting with the indicated antibodies(Cdc2, p-Cdc2, cyclinB) related to the cell cycle. Right panel: the results represent the mean (n = 3) ± SD of each group, and an asterisk (*) indicates a significant difference using Student's t-test. *p < 0.05 vs 0μM. D. A375 and Sk-Mel-28 cells were treated with various dosages of P22077 for 48h, and the apoptosis rate was determined by flow cytometry with Annexin V and PI double staining. The results represent the mean (n = 3) ± SD of each group and significant differences were evaluated using Student's t-test. *p < 0.05 vs 0μM. E. Western blotting was used to analyze MDM2, caspase-3 and cleaved-caspase-3 expression which related to cell apoptosis. Right panel: the results represent the mean (n = 3) ± SD of each group and significant differences were evaluated using Student's t-test. *p < 0.05 vs 0 μM.

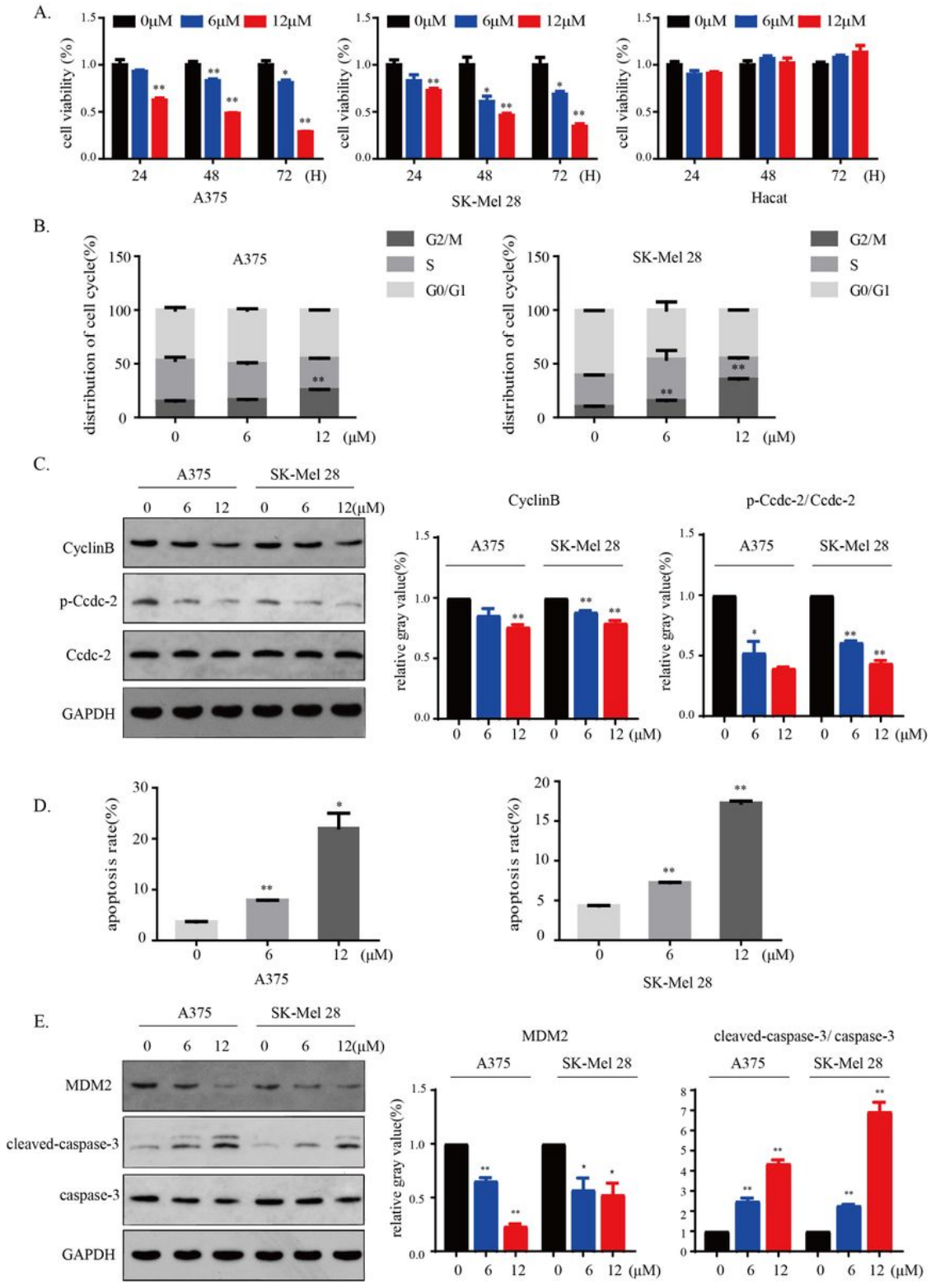

Figure 2

Pharmacological inhibition of USP7 by P22077 inhibits proliferation and induces cell cycle arrest and apoptosis in melanoma cells. A. The cell viability of melanoma cell lines in the presence or absence of USP7 inhibitor P22077. Cellsurvival was scored in triplicate normalized to control. Values are expressed asmean and SD from three independent experiments (*p<0.05, **p<0.01). B.A375 and Sk-Mel-28 cells were treated with different dosages of P22077 for 48h. The cell cycle distribution was detected by flow

cytometry. Significant differences were evaluated using Student's t-test. *p < 0.05 vs control. C. Whole cell lysates after treatment with the indicated concentration of P22077 were subjected to immunoblotting with the indicated antibodies(Cdc2, p-Cdc2, cyclinB) related to the cell cycle. Right panel: the results represent the mean (n = 3) ± SD of each group, and an asterisk (*) indicates a significant difference using Student's t-test. *p < 0.05 vs 0μM. D. A375 and Sk-Mel-28 cells were treated with various dosages of P22077 for 48h, and the apoptosis rate was determined by flow cytometry with Annexin V and PI double staining. The results represent the mean (n = 3) ± SD of each group and significant differences were evaluated using Student's t-test. *p < 0.05 vs 0μM. E. Western blotting was used to analyze MDM2, caspase-3 and cleaved-caspase-3 expression which related to cell apoptosis. Right panel: the results represent the mean (n = 3) ± SD of each group and significant differences were evaluated using Student's t-test. *p < 0.05 vs 0 μM.

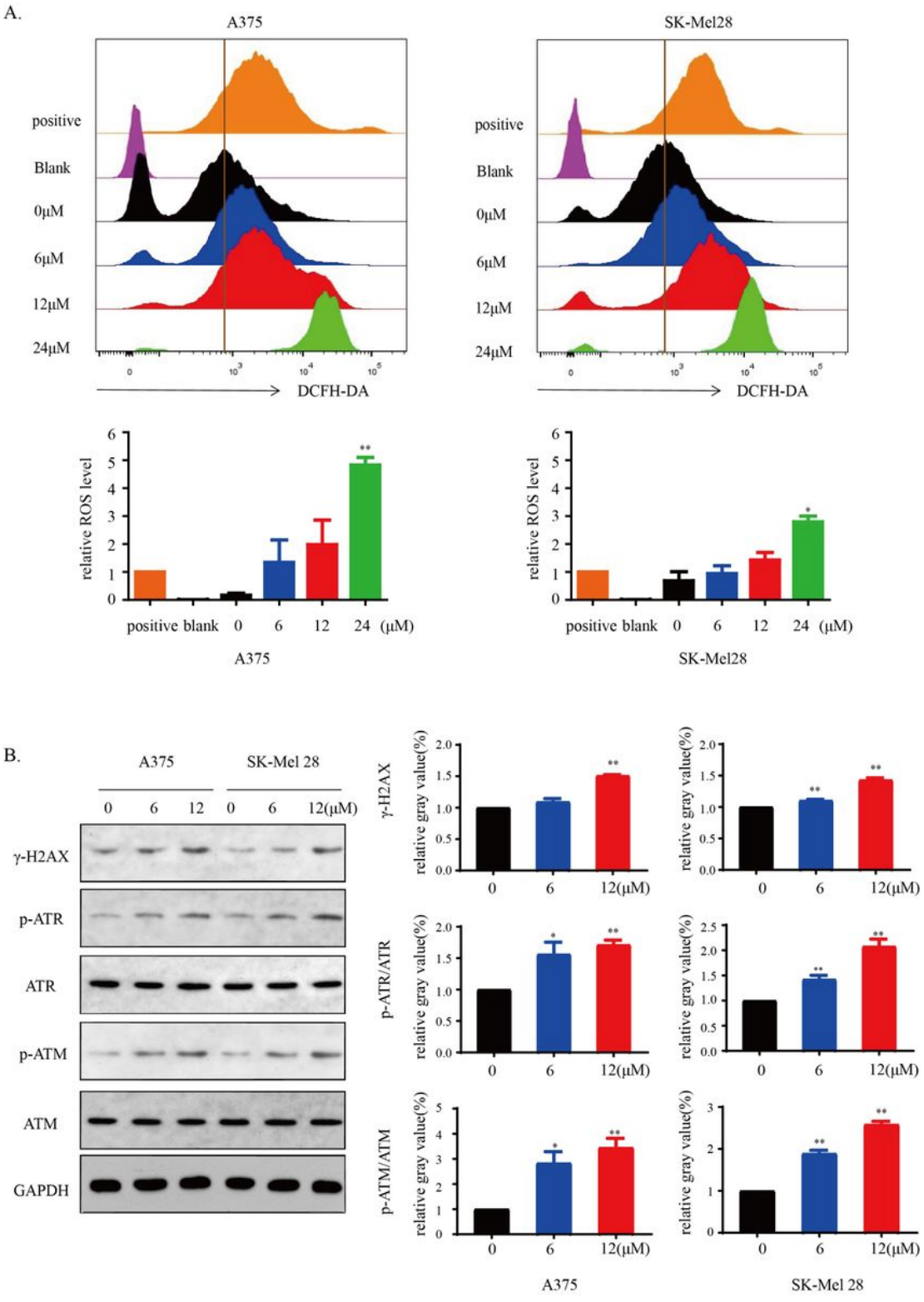

Figure 3

P22077 induced DNA damage by increasing the intracellular ROS level in melanoma cells. A. A375 and Sk-Mel-28 cells were exposed to P22077 or DMSO for 3h and then treated with 5 mmol/L N-acetylcysteine (NAC) for 30min. The levels of ROS were measured by DCF fluorescence with flow cytometry. The results represent the mean (n = 3) ± SD of each group and significant differences were evaluated using Student's t-test. *p < 0.05 vs 0μM(Lower panel). B. A375 and Sk-Mel-28 cells were treated

with P22077 for 48 h, and western blotting was performed for the indicated antibodies(ATM, p-ATM, ATR, p-ATR, γH2AX) related to DNA damage. Right panel: the results represent the mean (n = 3) ± SD of each group, and significant differences were evaluated using Student's t-test. *p < 0.05 vs 0 μM.

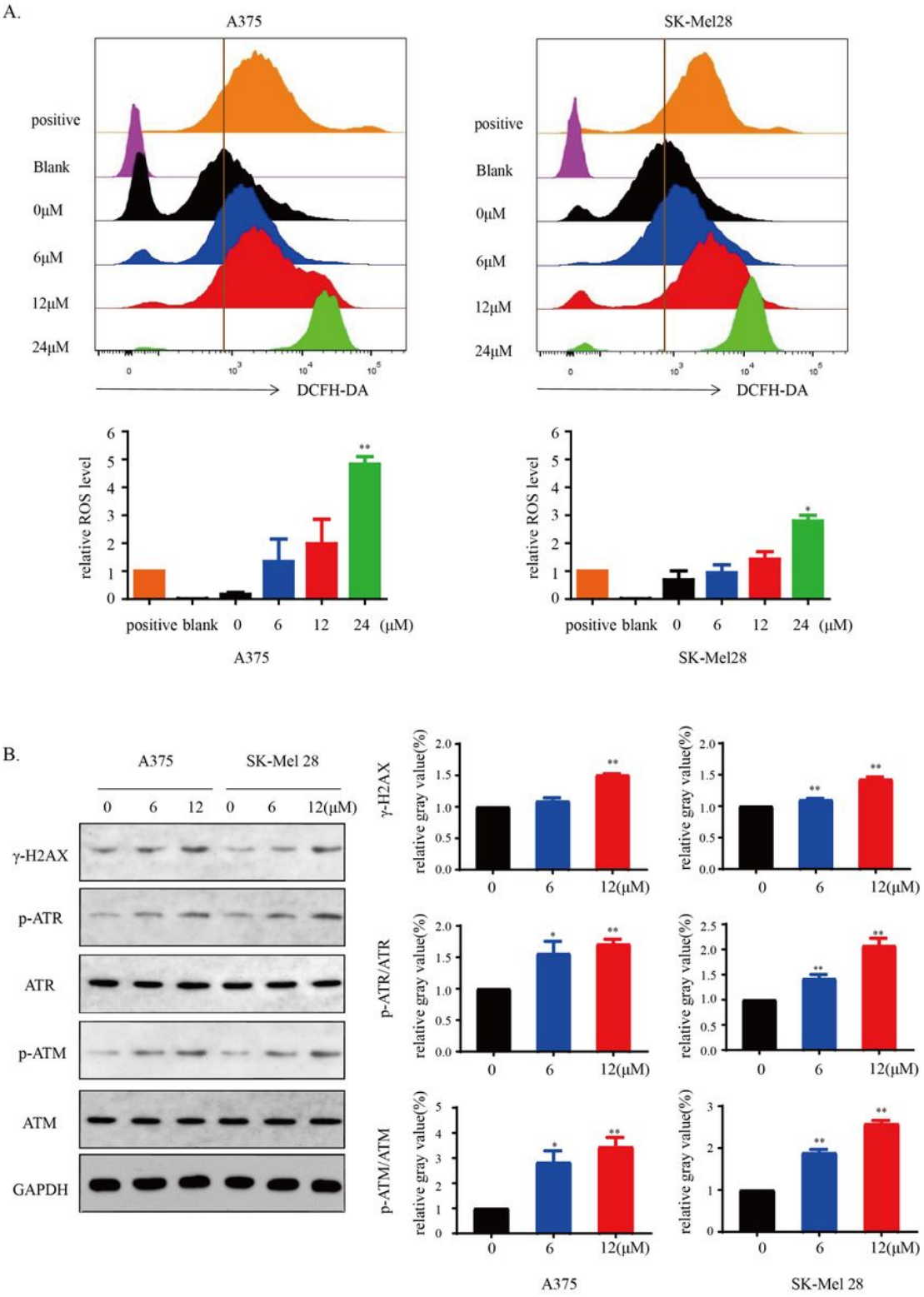

Figure 3

P22077 induced DNA damage by increasing the intracellular ROS level in melanoma cells. A. A375 and Sk-Mel-28 cells were exposed to P22077 or DMSO for 3h and then treated with 5 mmol/L N-

acetylcysteine (NAC) for 30min. The levels of ROS were measured by DCF fluorescence with flow cytometry. The results represent the mean (n = 3) ± SD of each group and significant differences were evaluated using Student's t-test. *p < 0.05 vs 0μM(Lower panel). B. A375 and Sk-Mel-28 cells were treated with P22077 for 48 h, and western blotting was performed for the indicated antibodies(ATM, p-ATM, ATR, p-ATR, γH2AX) related to DNA damage. Right panel: the results represent the mean (n = 3) ± SD of each group, and significant differences were evaluated using Student's t-test. *p < 0.05 vs 0 μM.

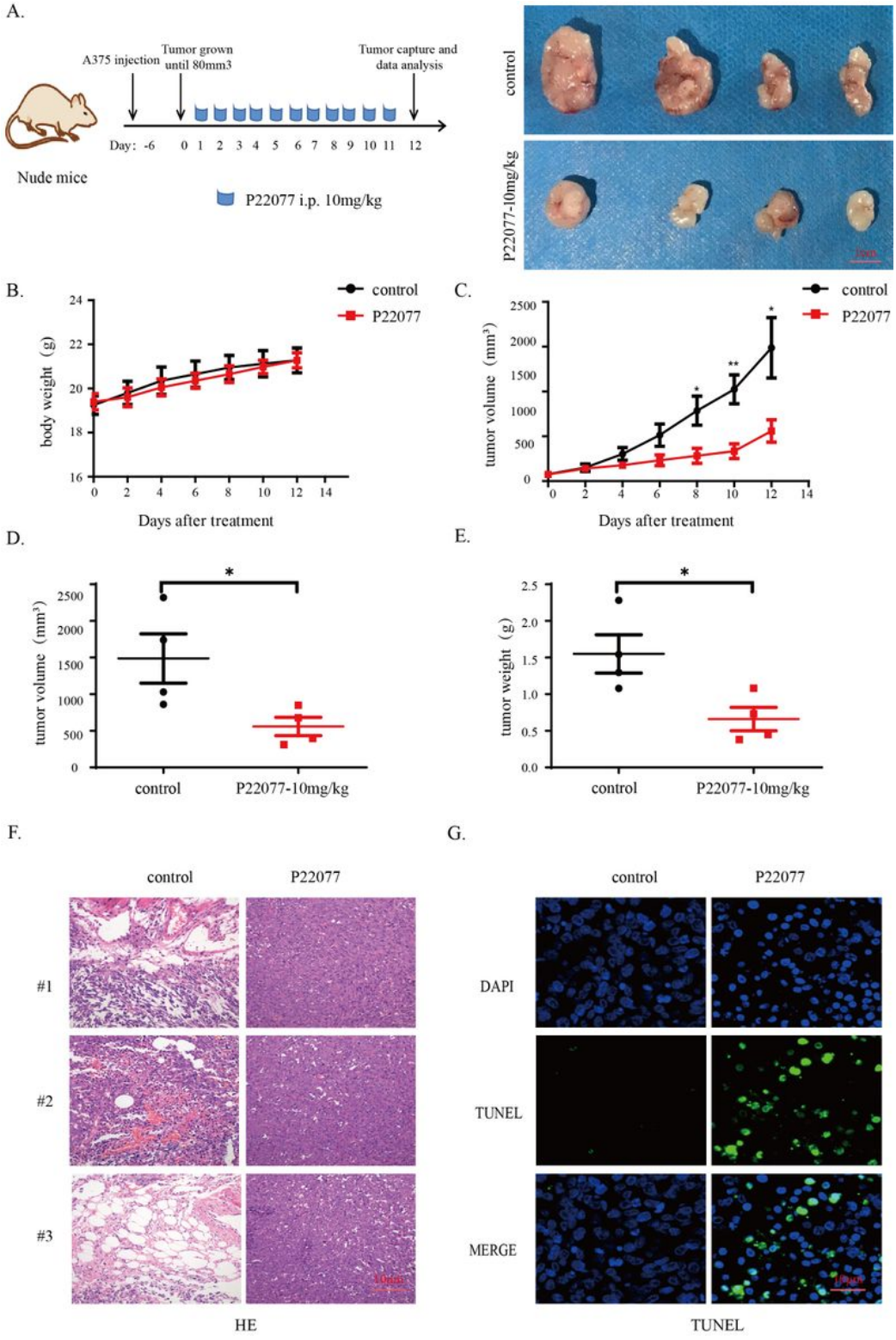

Figure 4

P22077 significantly inhibits melanoma tumor growth in vivo. A. A375 melanoma cells were xenografted into nude mice. The mice were randomized for intraperitoneal injection of P22077 (10mg/kg) or control as indicated time points for 12 days. Right panel: Photograph of the tumors from the mice after the mice were euthanized at the treatment end-point. The body weight (B) and tumor growth (C) were measured during the treatment period. (D and E)Tumors were removed at the treatment end-point and the volumes of each tumor mass from the mice were weighed (mean values ± SEM, n = 4). Significant differences were evaluated using a one-way ANOVA. *$p < 0.05$ vs control group. F.Tissue sections from the tumor were fixed and stained with HE (G) and TUNEL(F) to examine the tumor histochemical morphology of apoptosis. DAPI stained the nucleus. Scale bar is 50μm.

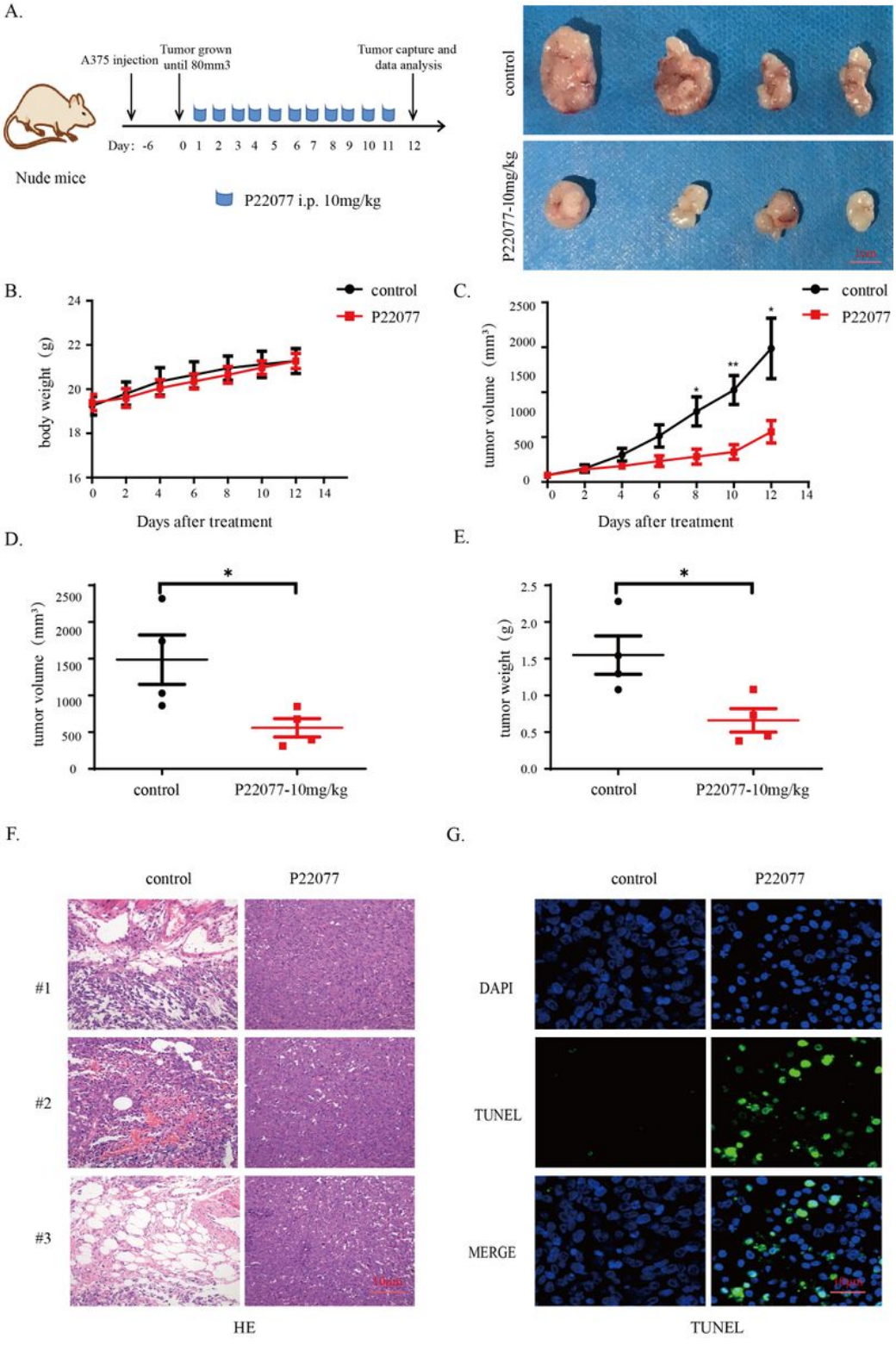

Figure 4

P22077 significantly inhibits melanoma tumor growth in vivo. A. A375 melanoma cells were xenografted into nude mice. The mice were randomized for intraperitoneal injection of P22077 (10mg/kg) or control as indicated time points for 12 days. Right panel: Photograph of the tumors from the mice after the mice were euthanized at the treatment end-point. The body weight (B) and tumor growth (C) were measured during the treatment period. (D and E)Tumors were removed at the treatment end-point and the volumes

of each tumor mass from the mice were weighed (mean values ± SEM, n = 4). Significant differences were evaluated using a one-way ANOVA. *p < 0.05 vs control group. F.Tissue sections from the tumor were fixed and stained with HE (G) and TUNEL(F) to examine the tumor histochemical morphology of apoptosis. DAPI stained the nucleus. Scale bar is 50μm.

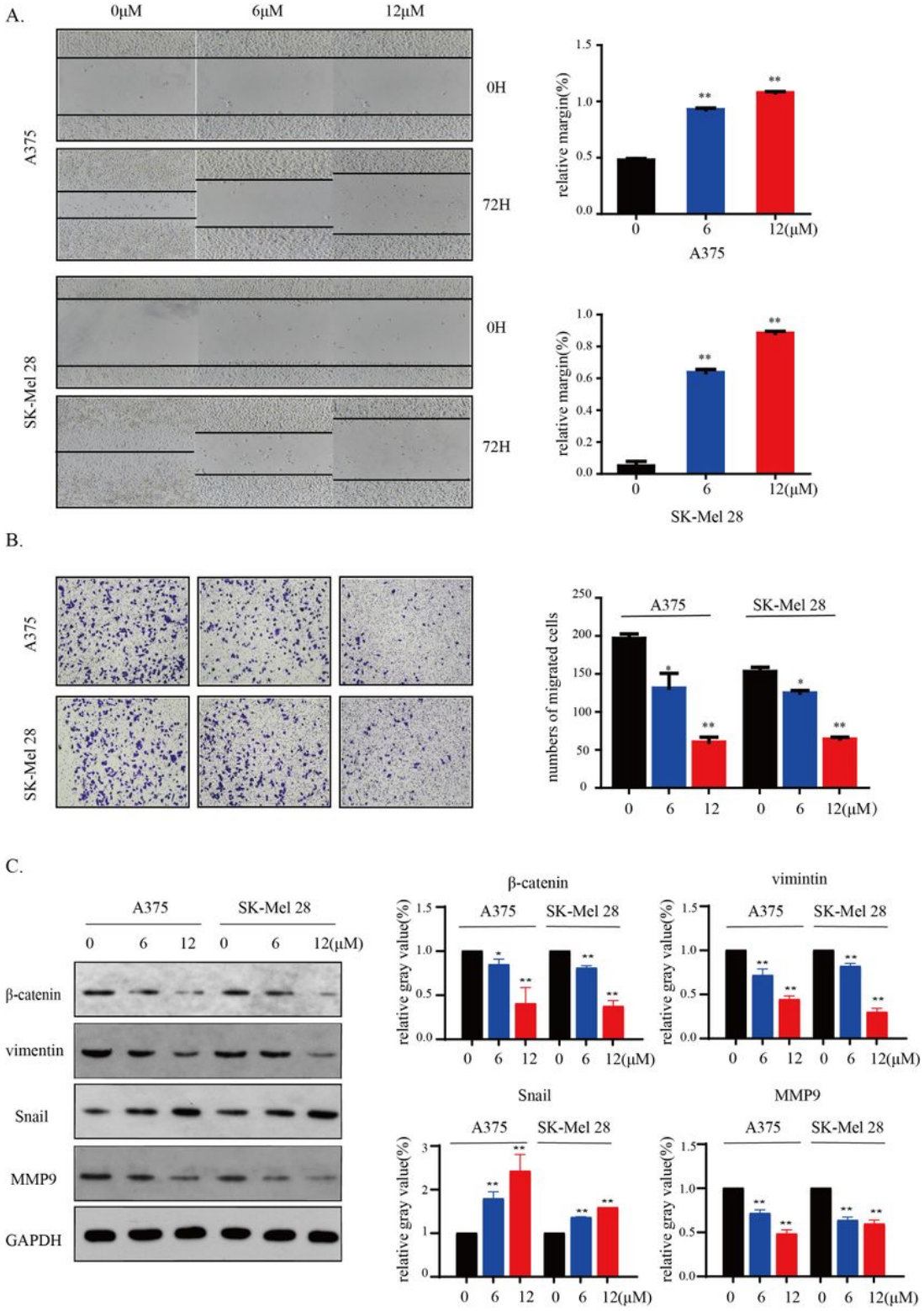

Figure 5

P22077 inhibits metastasis and invasion in melanoma cells. A. A375, Sk-Mel-28 cells were treated with various concentrations of P22077 or DMSO.Then the plates were scratch-wounded with a 200μl sterile pipette tip and then incubateThe healing was recorded with a phase-contrast microscope after 72H. Right panel:quantitative analysis of relative margin(%) (Mean values ± SEM, n = 3) Significant differences were evaluated using a one-way ANOVA. *p < 0.05 vs control. B. Transwell invasion assay determination of the number of melanoma cells that crossed the Matrigel layer after treated with P22077 or DMSO(Control).Right panel:the results represent the mean (n = 3) ± SD of each group, and significant differences were evaluated using Student's t-test. *p < 0.05 vs 0μM. C. A375 and Sk-Mel-28 cells were treated with P22077 for 48 h, and Western blotting analysis of the expression of metastasis markers (β-catenin, Vimentin, Snail, MMP9) .Right panel:the results represent the mean (n = 3) ± SD of each group, and significant differences were evaluated using Student's t-test. *p < 0.05 vs 0μM.

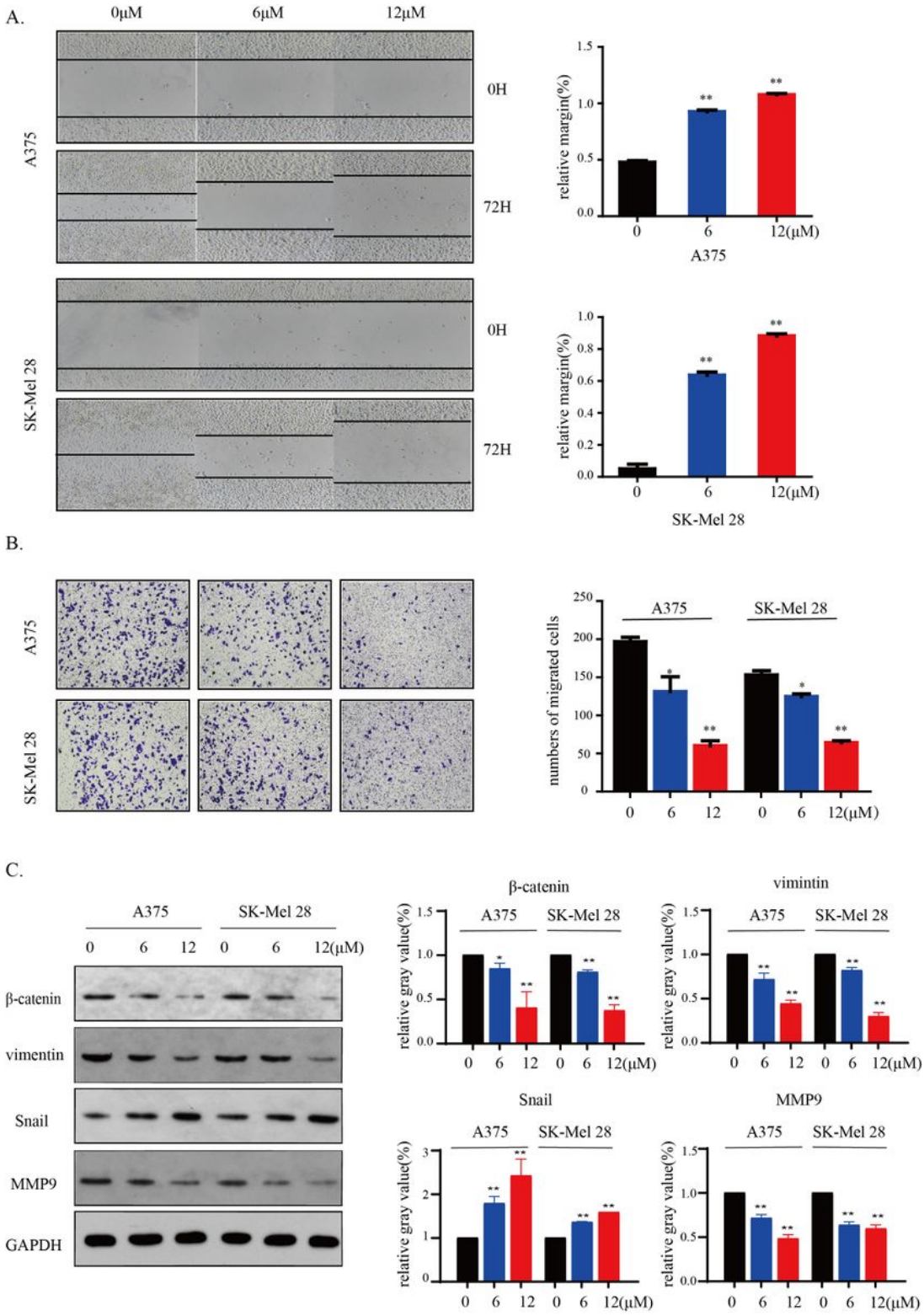

Figure 5

P22077 inhibits metastasis and invasion in melanoma cells. A. A375, Sk-Mel-28 cells were treated with various concentrations of P22077 or DMSO.Then the plates were scratch-wounded with a 200μl sterile pipette tip and then incubateThe healing was recorded with a phase-contrast microscope after 72H. Right panel:quantitative analysis of relative margin(%) (Mean values ± SEM, n = 3) Significant differences were evaluated using a one-way ANOVA. *p < 0.05 vs control. B. Transwell invasion assay determination of the

number of melanoma cells that crossed the Matrigel layer after treated with P22077 or DMSO(Control).Right panel:the results represent the mean (n = 3) ± SD of each group, and significant differences were evaluated using Student's t-test. *p < 0.05 vs 0μM. C. A375 and Sk-Mel-28 cells were treated with P22077 for 48 h, and Western blotting analysis of the expression of metastasis markers (β-catenin, Vimentin, Snail, MMP9) .Right panel:the results represent the mean (n = 3) ± SD of each group, and significant differences were evaluated using Student's t-test. *p < 0.05 vs 0μM.

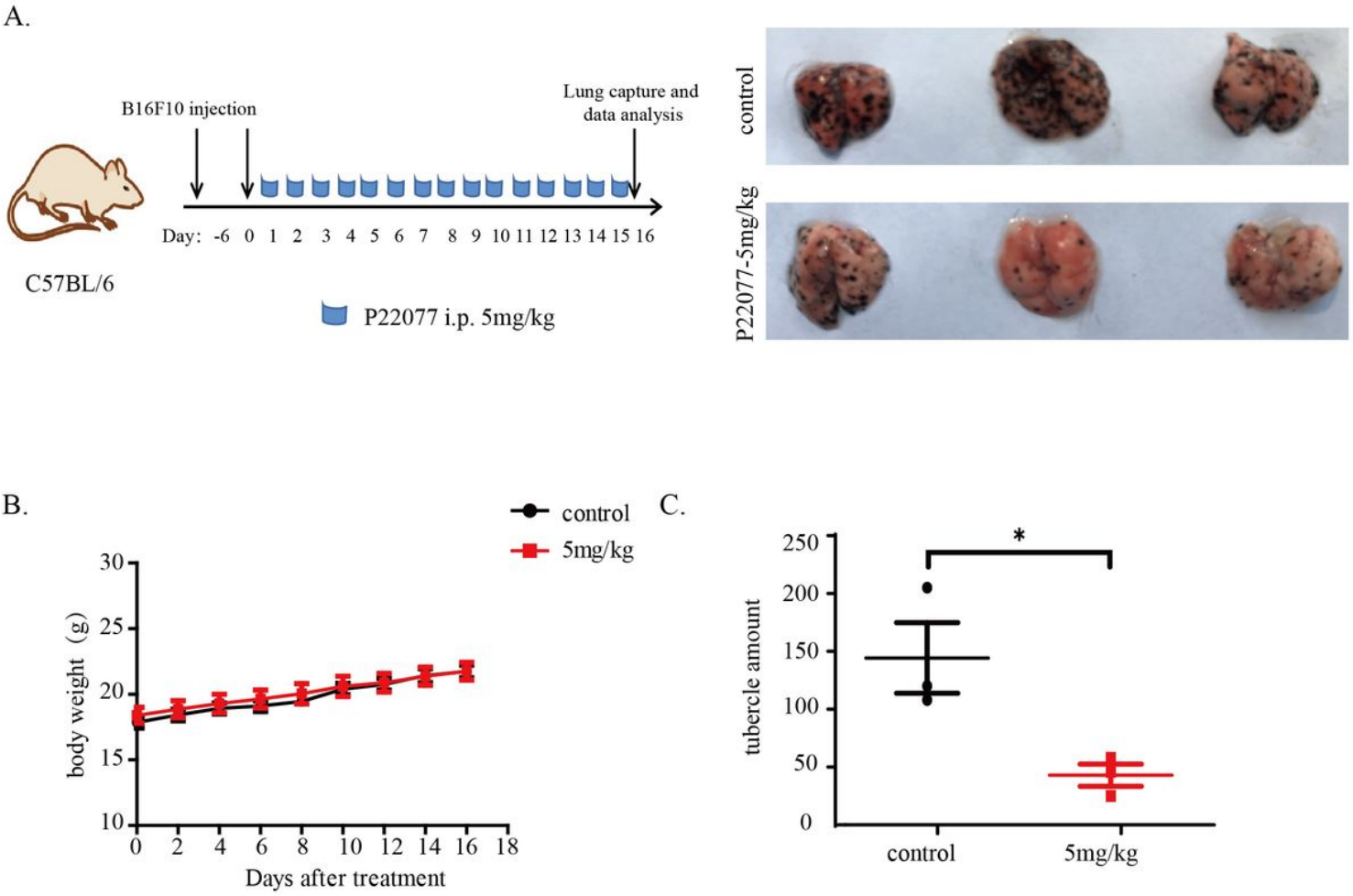

Figure 6

P22077 inhibits metastasis and invasion in vivo.A. melanoma cells from mice B16F10 were intramuscular injected into C57BL/6 mice. The tumor-bearing mice were randomized for intraperitoneal injection of P22077(5mg/kg) or control as indicated time points for 16 days. Representative photographs of Bouin-fixed lung specimens of mice injected with P22077 orvehicle.B. The body weight was measured during the treatment period. C.The nodules in lung tissue were counted and recorded. The results were shown as the mean tumor volume ± SD, and significant differences were evaluated using a one-way ANOVA. *p < 0.05 vs control. D. Proposed working model of P22077 on melanoma cells.

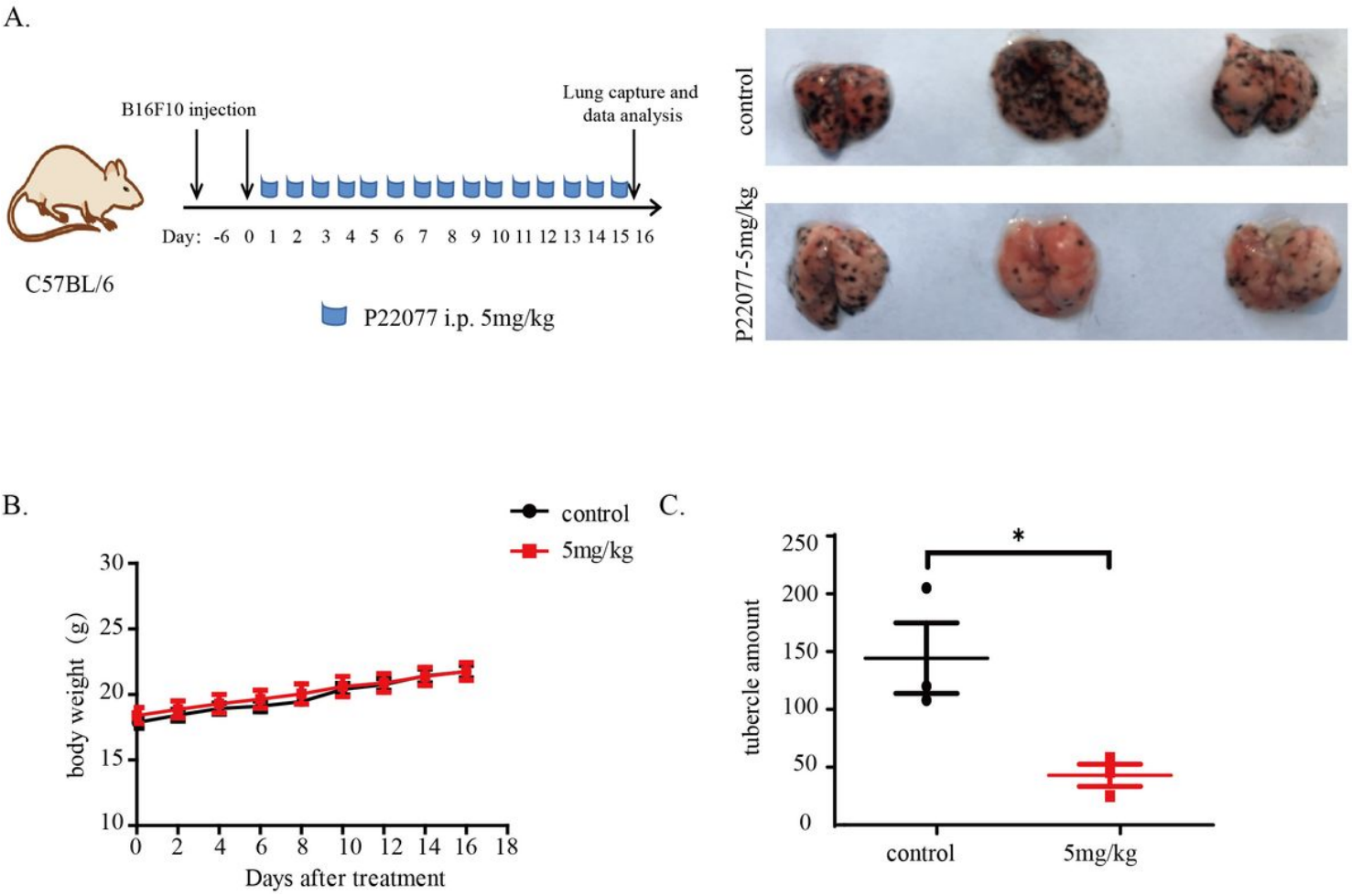

Figure 6

P22077 inhibits metastasis and invasion in vivo.A. melanoma cells from mice B16F10 were intramuscular injected into C57BL/6 mice. The tumor-bearing mice were randomized for intraperitoneal injection of P22077(5mg/kg) or control as indicated time points for 16 days. Representative photographs of Bouin-fixed lung specimens of mice injected with P22077 orvehicle.B. The body weight was measured during the treatment period. C.The nodules in lung tissue were counted and recorded. The results were shown as the mean tumor volume ± SD, and significant differences were evaluated using a one-way ANOVA. *p < 0.05 vs control. D. Proposed working model of P22077 on melanoma cells.

Supplementary Files

This is a list of supplementary files associated with this preprint. Click to download.

- supplement1.pdf
- supplement1.pdf

- supplement2.pdf
- supplement2.pdf